INVESTIGATION OF THE EFFECTS OF AGING ON THE ROOM AND HIGH TEMPERATURE TENSILE PROPERTIES AND FRACTURE OF STAINLESS STEEL 316L WELD METAL

Asadollah KARIMIYAN, Hassan FARHANGI and Ali Amari ALLAHYARI

School of Metallurgy and Materials Engineering, Faculty of Engineering, University of Tehran, Tehran, Iran.

ABSTRACT

In this research, variations of room and high temperature tensile properties and fracture behavior of 316L austenitic stainless steel weld metal as a function of aging temperature and time have been investigated. Stainless steel plates were welded using gas tungsten arc welding technique. Tensile test specimens of weld metal were subjected to various aging heat treatments at temperatures of 750 and 850°C for periods of 1 to 100 hours. Microstructural analyses were performed using techniques including metallography, EDS analysis, and measurement of ferrite content with ferritoscope. Fracture behavior of the weld metals was characterized by conducting tensile tests at 25 and 500°C, and performing fractographic and microstructural observations using SEM. Transformation of delta-ferrite to the intermetallic sigma phase during aging resulted in a mild increase in tensile strength and significant reduction in ductility. Slant and flat macroscopic fracture modes were observed in the aged weld metals, with the slant mode being dominant at 500°C. This mode was associated with deformation localization along arrays of primary voids, nucleated at cracked sigma phase particles, oriented at about 45° to loading direction. The transition in the fracture mode is further discussed based on variations in the dimpled fracture morphologies and strain hardening exponents.

Keywords: 316L weld metal, aging, dimpled fracture, flat fracture, slant fracture.

1. INTRODUCTION

Austenitic stainless steel alloys are used extensively in heat resistant structural components in power generating and chemical industries due to their metallurgical stability, excellent corrosion resistance, and good creep strength and ductility properties at elevated temperatures [1-3]. It has been established that successful welding of this type of stainless steel requires the presence of at least 5%, by volume, of δ-ferrite in the microstructure [2-4]. The ferrite is beneficial because it restricts grain growth and prevent liquid cracking by limiting impurity element diffusion and inhibiting wetting of liquid films [1,2]. During post weld heat treatment or high temperature exposure as encountered in service, the ferrite transforms to a variety of secondary phases such as M23C6 carbides as well as the intermetallic phases such as σ and χ [4-7]. These phases are known to degrade the mechanical and corrosion properties of the weld metal [4]. However, the formation of these phases is influenced by a number of factors such

as weld metal composition, ferrite content and its morphology, in addition to temperature and time of transformation [4]. The mechanical properties of δ-ferrite containing weld metals are generally controlled by the kinetics of δ-ferrite dissolution, as well as the nature of transformation products [7]. Therefore, transformation kinetics and its subsequent effects on mechanical properties has been the subject of many studies [5-7]. In this research, variations of room and high temperature tensile properties and fracture behavior of 316L austenitic stainless steel weld metal as a function of aging temperature and time have been investigated. Rapid dissolution of δ-ferrite and formation of a brittle sigma phase network during high temperature aging promote changes in tensile properties, fracture mode and morphology.

2. EXPERIMENTAL PROCEDURE

Using the gas tungsten arc welding process, type 316L stainless steel filler wire were deposited in a weld geometry shown in Figure 1 and described by ISO2560. The steel plates used were 15 mm thick 316L stainless steel dimensioned 1000 × 110 mm. The chemical composition of the weld metal and the welding parameters are given in Table 1 and Table 2, respectively. All welded sections were subjected to nondestructive examinations including ultrasonic and radiographic testing for quality control prior to sample preparation.

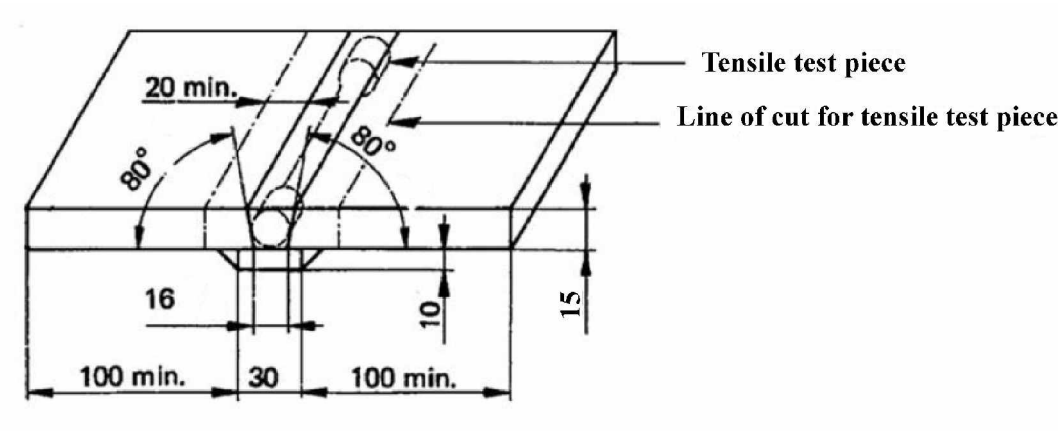

Figure 1. Welding geometry and location of weld metal tensile test specimen.

Table 1. Chemical composition of 316L austenitic stainless steel weld metal

Alloy type	Composition (wt. %)									
316 L weld metal	C	Cr	Ni	Mo	Mn	Co	Al	P	Cu	Fe
	0.017	17.16	10.22	2.18	1.19	0.13	0.004	0.03	0.23	balance

Table 2. Welding parameters

Electrode Diameter	3.2 mm	**Argon Flow Rate**	8.5l Lit/min
Welding Current	130 A	**Shielding Gas**	Ar 99.99 %
Welding Wire	AISI 316L	**Polarity**	DCEN
Welding Wire Diameter	2.4 mm	**Welding Speed**	1 cm/min

Round shape weld metal tensile specimens were machined from the welded sections shown in Figure 1 and subsequently aged at 750 and 850 °C, for durations of 1, 5, 25, and 100 hours. Tensile tests were carried out at a nominal strain rate of 5×10-4 s-1 on the unaged and aged weld metals at temperatures of 25 and 500 °C. The ferrite content in the weld metal was measured before and after aging using ferritoscope, which was calibrated with a magnetic probe, in accordance with the procedure laid down in AWS A4.2-74. Microstructural observations were conducted using optical and scanning electron microscopes, after etching the weld metal specimens in Murakami's reagent. Chemical composition of constituent phases was analyzed using energy dispersive spectroscopy. Fractographic examinations of tensile fracture surfaces were carried out using SEM.

3. RESULTS AND DISCUSSION

3.1 Microstructure

Typical optical micrograph of the microstructure of unaged weld metals is shown in Figure 1(a). The microstructure of unaged weld metal in Figure 1(a) exhibits characteristics of dual phase structures consisting of white austenite matrix and dark delta-ferrite as a secondary phase. The duplex microstructure is a consequence of incomplete $\delta \rightarrow \gamma$ transformation during solidification of weld metal. It can be observed that most of δ-ferrite has been consumed in the transformation, but a residual skeletal core of δ-ferrite, schematically shown in Figure 1(b) is retained in the as-welded microstructure. Due to its inherent microstructural instability, δ-ferrite undergoes a progressive dissolution at high aging temperatures of 750 and 850 ºC which leads to the formation of a skeletal network of sigma phase particles. Based on measurements of δ-ferrite content using ferritoscope, the average δ-ferrite content of the 316L weld metal in this study was found to be 7.5 FN. The percentages of ferrite transformed as a function of aging time are shown in Figure 2(a).

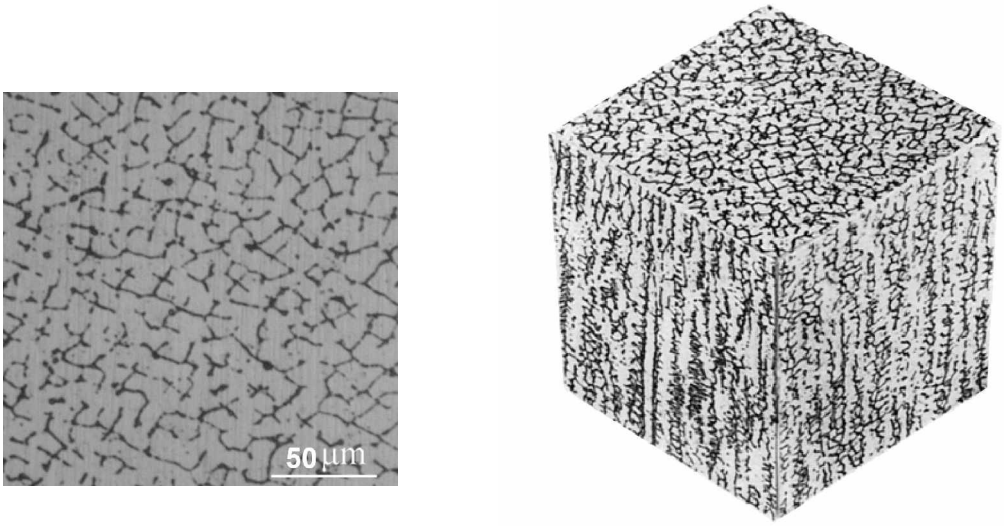

(a) (b)

Figure 1. (a) The microstructure of unaged weld metal**,** (b) schematic 3-D view of the residual skeletal core of δ-ferrite in the weld metal [8].

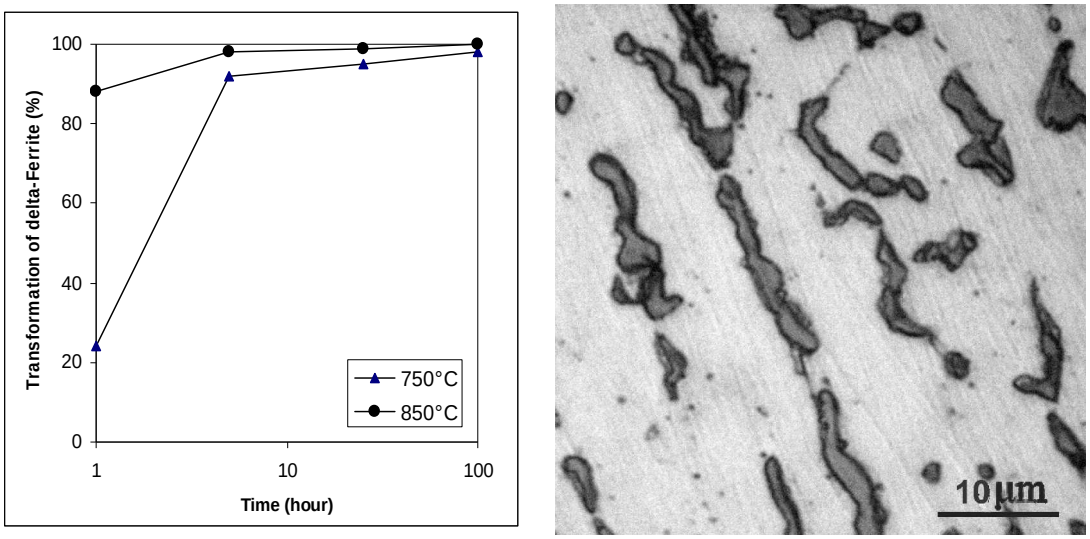

(a) (b)

Figure 2. (a) The percentages of ferrite transformed as a function of aging time, (b) optical micrograph showing sigma phase particles after aging for 100 h at 850 ºC.

At the aging temperatures of 750 and 850 ºC investigated, nearly full transformation of δ-ferrite takes place within a short period of time, so that the time required for 90% transformation is about 1 hour and 5 hours, respectively. Figure 2(b) shows the sigma phase particles after aging for 100 h at 850 ºC. The skeletal network of sigma phase is more or less continuous at lower aging times but prolonged aging at these temperatures leads to partial and localized spherodization of sigma phase which progresses by necking of elongated, unstable sigma particles and formation of smaller particles with more equilibrium shapes [5].

3.2 Tensile Properties

Tensile tests were carried out at 25 °C and 500 °C. The percentage changes in tensile strength and tensile ductility, i.e., percent elongation, of aged weld metals compared to the unaged weld metal at both testing temperatures are shown in Figure 3(a,b). In general, aging causes a mild increase in tensile strength. The increase in tensile strength reaches its maximum after 5 and 25 hours of aging at 850 °C at tensile test temperatures of 25 and 500 °C, respectively.

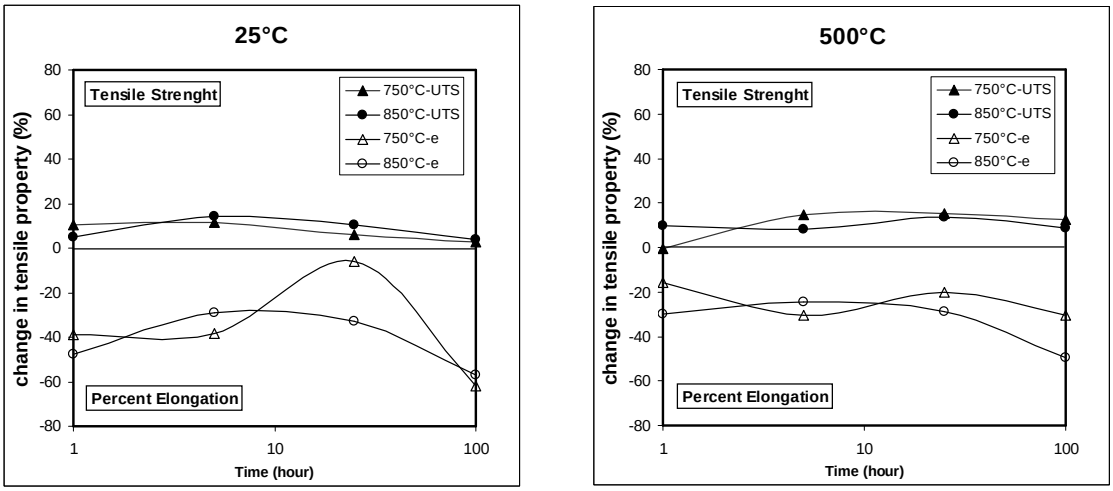

(a) (b)

Figure 3. The percentage changes in tensile properties due to aging.

On the other hand, the tensile ductility of the weld metal is considerably reduced due to aging. The reduction tends to be larger at higher aging temperatures and times. However, the curves for changes in ductility at aging temperatures of 750 and 850 °C exhibit maximum points. The time required to reach the maximum point decreases from 25 to 5 hours with increasing aging temperature for both tensile testing temperatures.
The mild increase in tensile strength and the significant reduction in tensile ductility of the aged weld metals can be attributed to formation of the brittle intermetallic sigma phase network. The partial spherodization of sigma phase seems to temporarily arrest and even partly compensate the loss in tensile ductility. This effect can be deduced from the occurrence of maximum points on the change in ductility curves. In as much as the progress of spherodization is faster at higher aging temperatures, the maximum point on the change in ductility curve is displaced to lower aging times at 850 °C, accordingly.

3.3 Fracture modes

The unaged weld metal exhibited cup and cone mode of fracture at both tensile testing temperatures. However macroscopic fracture surfaces of aged weld metals exhibited two distinct fracture modes, including slant and flat fractures (Figure 4). In the slant fracture mode the macroscopic fracture surface remained inclined roughly at 45° angle with respect to the loading direction, whereas in the flat fracture mode the fracture surface orientation was roughly normal to the loading direction. The slant fracture mode was dominant at 500 °C regardless of aging temperature and time. This fracture mode was also dominant at 25 °C for weld metals aged at 750 °C for durations of up to 25 hours. However, increasing aging time or temperature induced a change from the slant to the flat fracture mode.

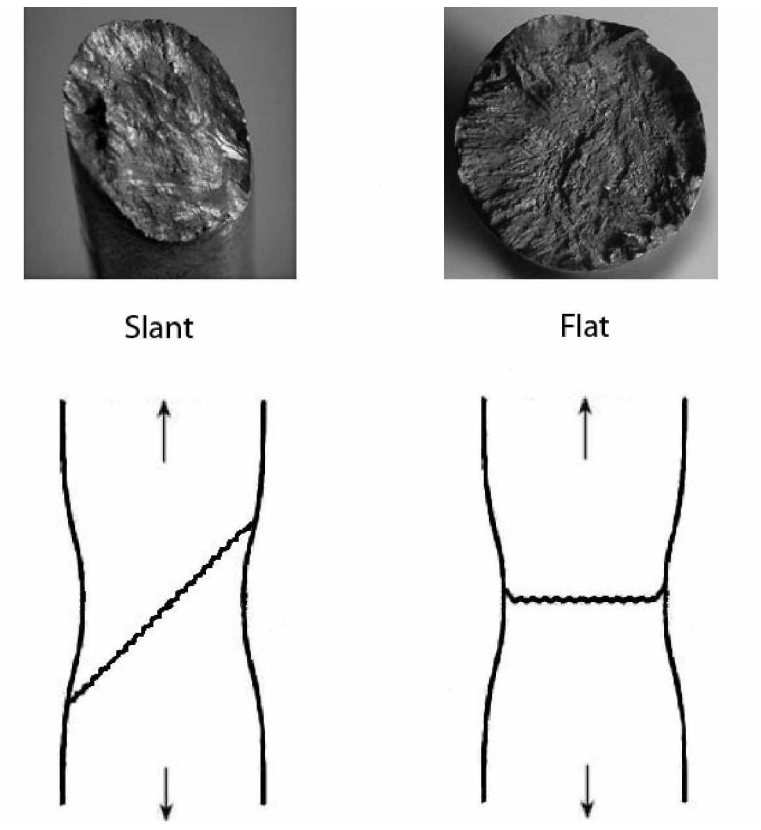

Figure 4. Slant and flat fracture modes.

Typical micrographs of regions directly beneath the slant fracture surfaces of aged weld metals are shown in Figure 5(a,b). It can be seen that the fracture process occurred in a manner that created a zig-zag profile comprised of segments oriented roughly 45° to the loading direction. A row of primary voids, aligned roughly parallel to the slant fracture surface can also be observed in Figure 5(a). Parallel arrays of primary voids inclined at 45° to the loading direction are shown in a higher magnification micrograph in Figure 5(b). It is clear that the primary voids nucleated at cracked sigma phase particles. These particles can thus be identified as the primary microstructural factor responsible for fracture initiation. Preferential growth of primary voids on planes oriented at 45° to the loading direction is indicative of the deformation localization process that occurred between the primary voids, leading to failure by a void-sheet mechanism.

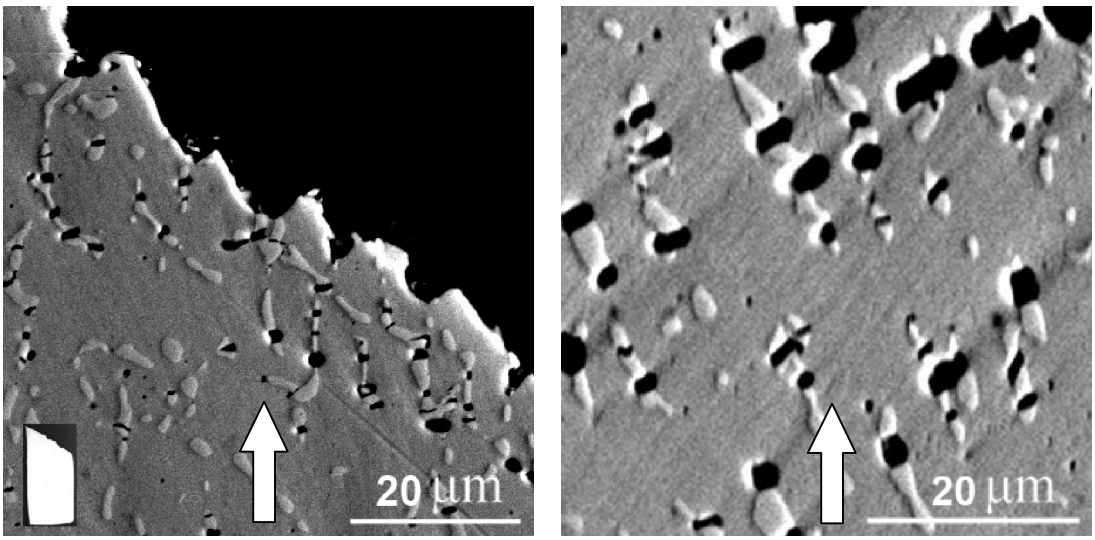

(a) (b)

Figure 5. SEM micrographs of (a) slant fracture surface profile and (b) inclined parallel arrays of primary voids in aged weld metals. Arrows show the loading direction.

Slant fracture modes have previously been shown to occur in a wide rang of alloys including some aluminum alloys [9,10], Cr-Mo-V steel [10], and HY100 steel [11,12]. Second phase particle distributions in the form of stringer or elongated inclusion patterns have been shown to play a key role in promoting slant fracture mode [9,11,12]. These types of particles nucleate elongated voids which are able to induce deformation localization and void-sheet coalescence over an extended scale within the microstructure [11,12] . Presence of elongated voids can perturb the far-field stress state locally such that the intervoid ligament experiences plane-strain deformation between the primary voids. Particularly if the primary voids are located at either 45° or 30° to the loading direction intense strain localization occurs. In the aged weld metal microstructures investigated in this research the primary voids were shown to be associated with the sigma phase network which mainly consists of interconnected branches of elongated particles in a skeletal type of distribution.

One of the key material parameters which have been shown to affect the transition from slant fracture to flat fracture mode is the strain hardening exponent [9,12]. Condition of band localization is more easily fulfilled and favored by a low strain hardening exponent. The strain

hardening exponents of aged weld metals, obtained from the true stress-true strain curves using the Holloman relationship [13], at 25 and 500 °C are shown in Figure 6.

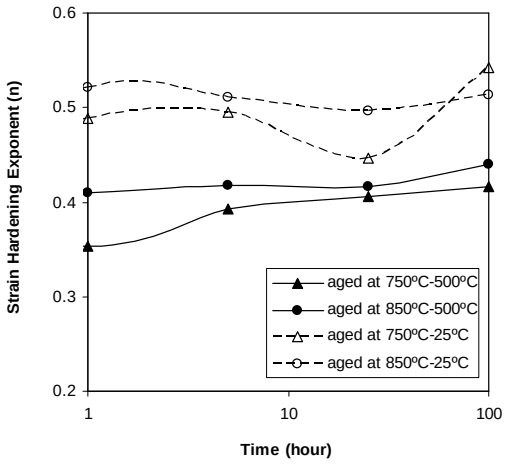

Figure 6. Strain hardening exponents of aged weld metals

At room temperature the weld metals aged at 750 °C for duration of up to 25 hours exhibit a lower strain hardening exponent which promotes a slant mode of fracture. However increasing aging time or temperature raise the strain hardening exponent leading to a flat fracture mode. At 500 °C, the strain hardening exponent of all of aged weld metals drops considerably compared to room temperature. As a result the slant mode of fracture dominates the fracture process at this temperature.

3.4 Fracture surface morphology

The dominant failure mechanism in aged and unaged weld metals was ductile rupture by void initiation, growth, and coalescence. Accordingly, the fracture surfaces exhibited a dimpled morphology, as shown in Figure 7(a,b). However, the size, shape and distribution of dimples was affected by the aging heat treatment and the macroscopic fracture modes of specimens.

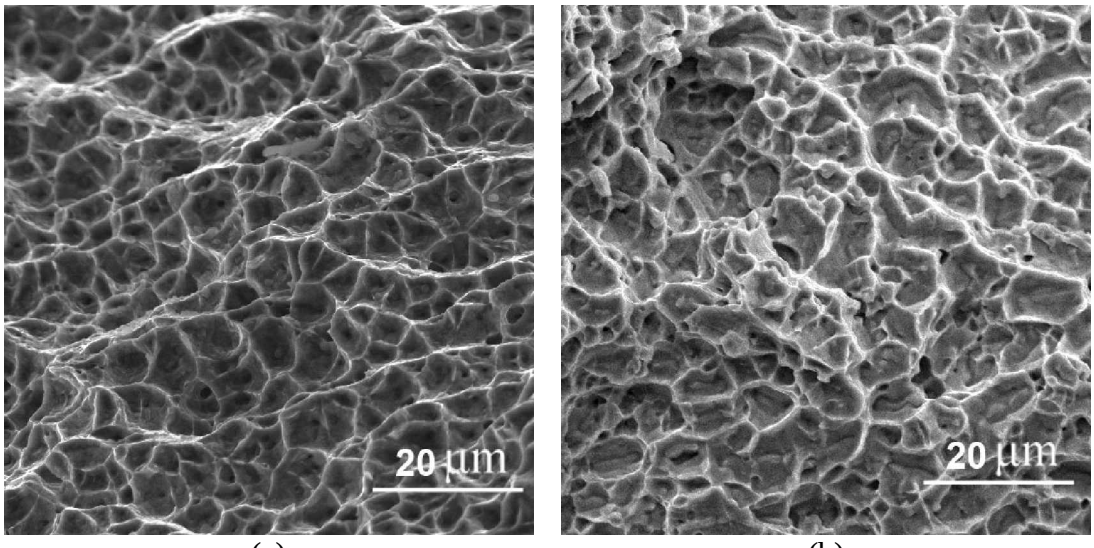

(a) (b)

Figure 7. SEM Fractographs of dimpled fracture morphologies in (a) unaged weld metal (b) aged weld metal with a slant fracture mode.

In the unaged weld metals which exhibit cup and cone type fracture the roughly equiaxed dimples which nucleated at inclusions have a more uniform distribution with an average size of about 5 μm (Figure 7(a)). In the slanted plane of fracture in aged weld metals the dimples seem to exhibit a dual size distribution (Figure 7(b)). Large and shallow voids which nucleate at sigma phase particles, and are typically larger than 10 μm in size, are partly separated by local distributions of much finer voids at some outer boundaries. This dual distribution of voids is indicative of failure by void-sheet mechanism. The effect of local clusters of sigma phase particles is more evident on the flat fracture surface of aged weld metals. Brittle fracture of these clusters leads to extensive secondary crack formation as shown in Figure 8.

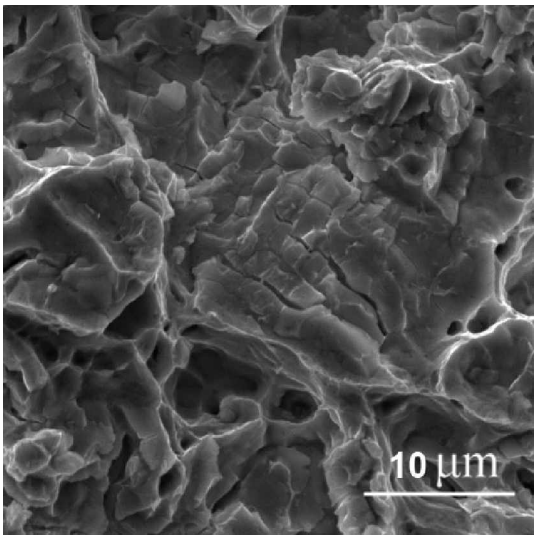

Figure 8. SEM fractograph of secondary crack formation as a result of brittle fracture of sigma phase clusters in aged weld metal with a flat fracture mode.

4. CONCLUSIONS

1- At the aging temperatures of 750 and 850 °C investigated, the skeletal delta ferrite is rapidly replaced by a network of brittle sigma phase particles, which cause a mild increase in tensile strength and a significant reduction in tensile ductility.
2- The macroscopic fracture mode of the aged weld metals is either slant or flat, with the slant mode being dominant at tensile testing temperature of 500 °C, whereas the weld metal exhibits a cup and cone type fracture.
3- The slant fracture mode in the aged weld metals is associated with deformation localization along arrays of primary voids nucleated at cracked sigma phase particles and oriented at about 45° to the loading direction, which promote a void-sheet mechanism.
4- The change from slant to flat mode of fracture at room temperature seems to be related to an overall increase in the strain hardening exponent with aging time and temperature.

ACKNOWLEDGEMENTS
The authors are grateful for helpful assistance of Mr. S.A. Eftekhari, and Eng. F. Hassanabadi during the study.

REFERENCES

1. Mills, W., “Fracture toughness of type 304 and 316 stainless steels and their welds”, International Material Reviews, Vol. 42, No. 42, pp. 45-82, 1997.
2. Smith, J.J. and Farrar, R.A., “Influence of microstructure and composition on mechanical properties of some AISI 300 series weld metals”, International Materials Reviews, Vol. 33, No. 1, pp. 25-51, 1993.
3. Song, Y., Baker, T.N., McPherson, N.A., “A study of precipitation in as-welded 3 16LN plate using 316L/317L weld metal”, Materials Science and Engineering, A212, pp. 228-234, 1996.
4. Gill, T.P.S., Shankar, V., Pujar, M.G., Rodriguez, P., “Effect of composition on the transformation of δ-ferritr to σ in type 316 stainless steel weld metals”, Scripta Metallurgica et Materialia, Vol. 32, No. 10, pp. 1595-1600, 1995.
5. Gill, T.P., and Vijayalakshmi, M., “On microstructure-property correlation of thermally aged type 316L stainless steel weld metal”, Metallurgical Transactions, Vol. 20A, pp. 1115-1124, 1989.
6. Farrar, R.A., "The importance of microstructural transformations for welding and the stability of long term service properties", Welding In the World, 36, 143-151, 1995.
7. Smith, J.J., “Effect of composition on the transformation behavior of duplex 316 weld metal”, Journal of Material Science, Vol. 26, pp. 5025-5036, 1991.
8. Piatti, G., Vedani, M., “Relation between tensile properties and microstructure in type 316 stainless steel SA weld metal”, Journal of Materials Science, vol. 25, pp. 4285-4297, 1990.
9. Metzger, D.R., Duan, X., Jain, M., Wilkinson, D.S., Mishra, R., Kim, S., Sachdev, A.K., “The influence of particle distribution and volume fraction on the post-necking behaviour of aluminium alloys”, Mechanics of Materials, vol. 38, pp. 1026–1038, 2006.
10. Asserin-Lebert, A., Besson, J., Gourgues, A.F., “Fracture of 6065 aluminum sheet materials: effect of specimen thickness and hardening behavior on strain localization and toughness”, Materials Science and Engineering A, A395, pp. 186-194, 2005.
11. Bandstra, J.P., Koss, D.A., ”Modeling the ductile fracture process of void coalescence by void-sheet formation”, Materials Science and Engineering, A319, pp. 490–495, 2001.
12. Bandstra, J.P., Koss, D.A., Geltmacher, A., Matic, P., Everett, R.K., “Modeling void coalescence during ductile fracture of a steel”, Materials Science and Engineering A, A366, pp. 269-281, 2004.
13. Dieter, G., **Mechanical Metallurgy**, 3rd edition, Mc Graw Hill, 2001.